ЗАБАБАХИНСКИЕ 2017 НАУЧНЫЕ ЧТЕНИЯ

On similarity of dynamic failure processes in metals of various geometry at different time-amplitude characteristics of external action

Kosheleva E.V., Selchenkova N.I., Sokolov S.S., Trunin I.R., Uchaev A.Ya.

Russian Federal Nuclear Center – VNIIEF, Sarov, Russia
E-mail: uchaev@expd.vniief.ru

$$dE = TdS - PdV$$

$$\frac{T}{dV} = \frac{P}{dS}$$

$$P < 0, \quad dV < 0$$

$$K \sim \left(dP / d\rho \right)_T = 1/\chi$$

Loading parameters

$$\frac{dJ}{dm} \geq 10^{13}$$

Time-temperature regularities of dynamic failure process under the action of REB and LR

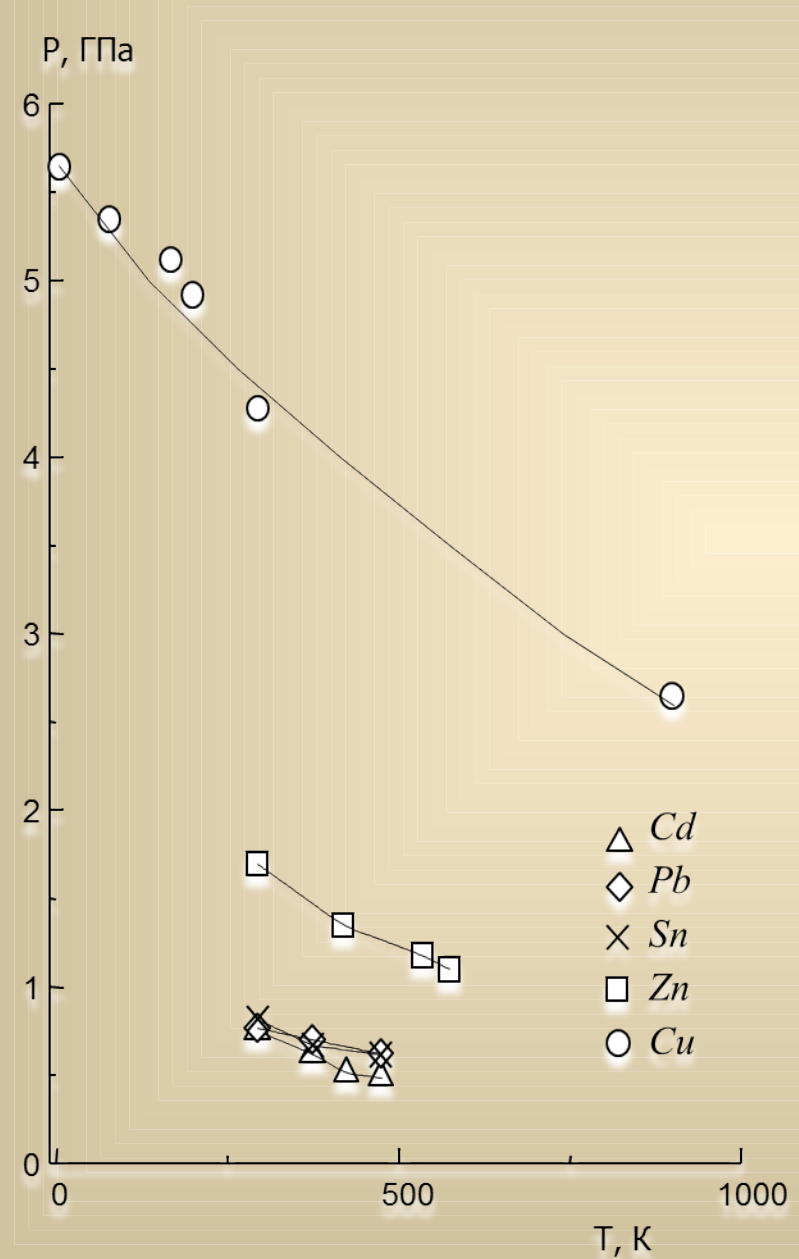

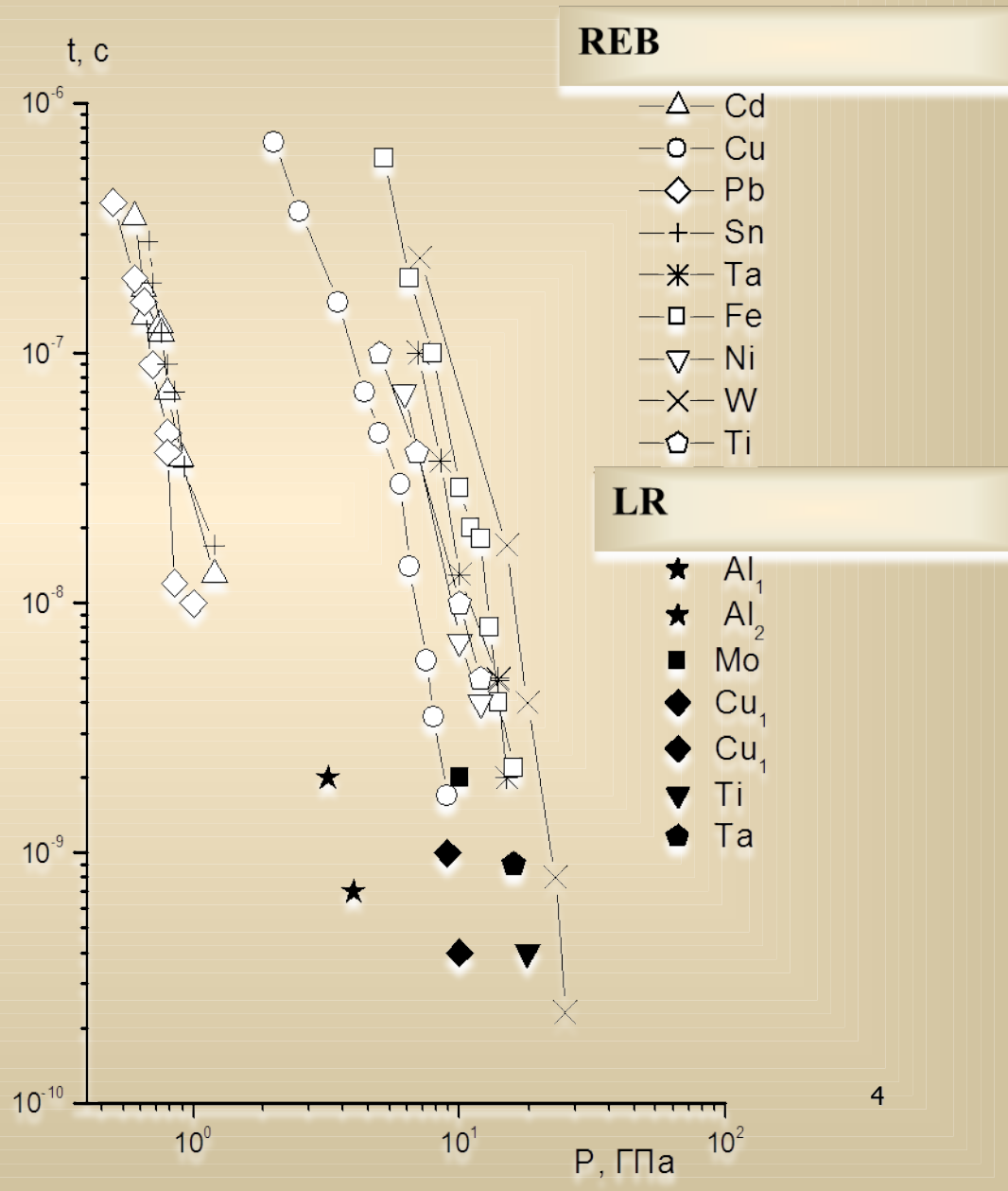

Structurization of the lattice slip bands near the growing fracture centers and tangents to the slip bands

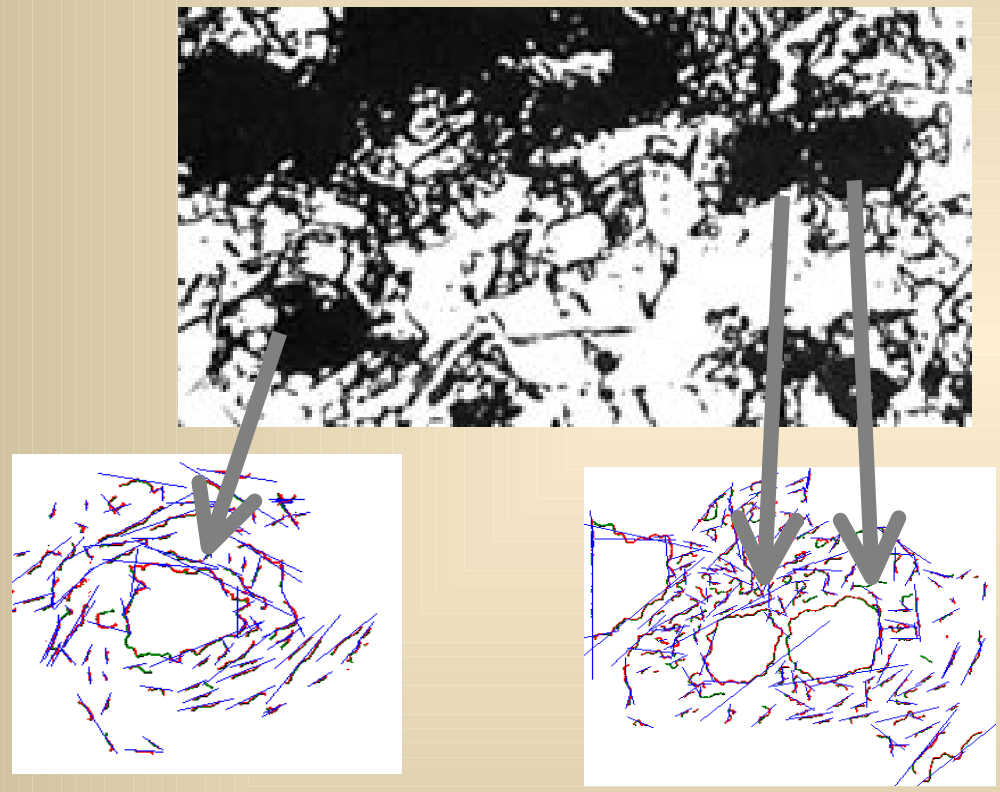

Size distribution of fracture centers in *Fe* ($\Delta=4\cdot10^{-4}$m) and *Cu* ($\Delta=10^{-3}$m) samples

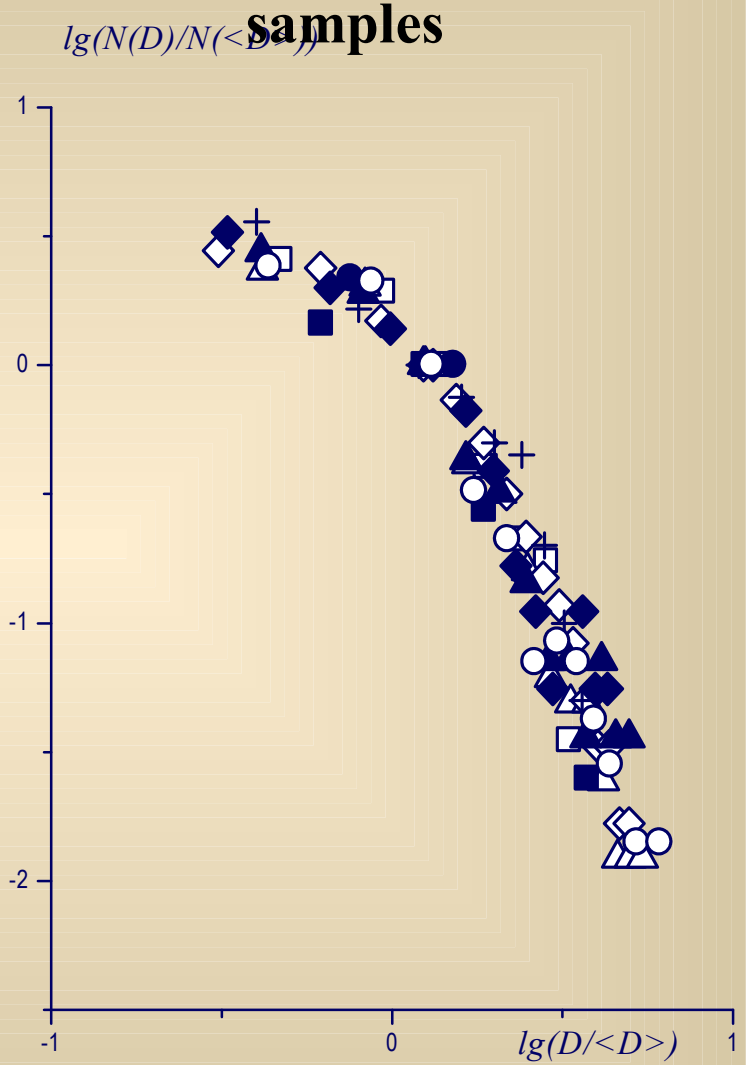

Bitmapped images of patterns of gravitation turbulent mixing of two incompressible various density liquids (three layers at different height from the liquid-liquid interface $h_1 < h_2 < h_3$)

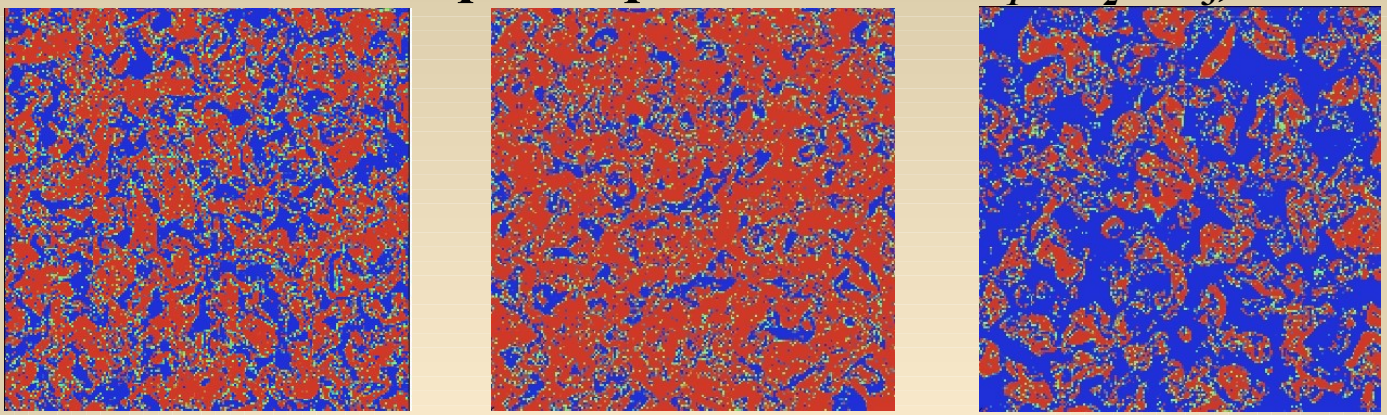

h_1 h_2 h_3

Examples of similarity of origin for various nature infinite clusters near the critical point

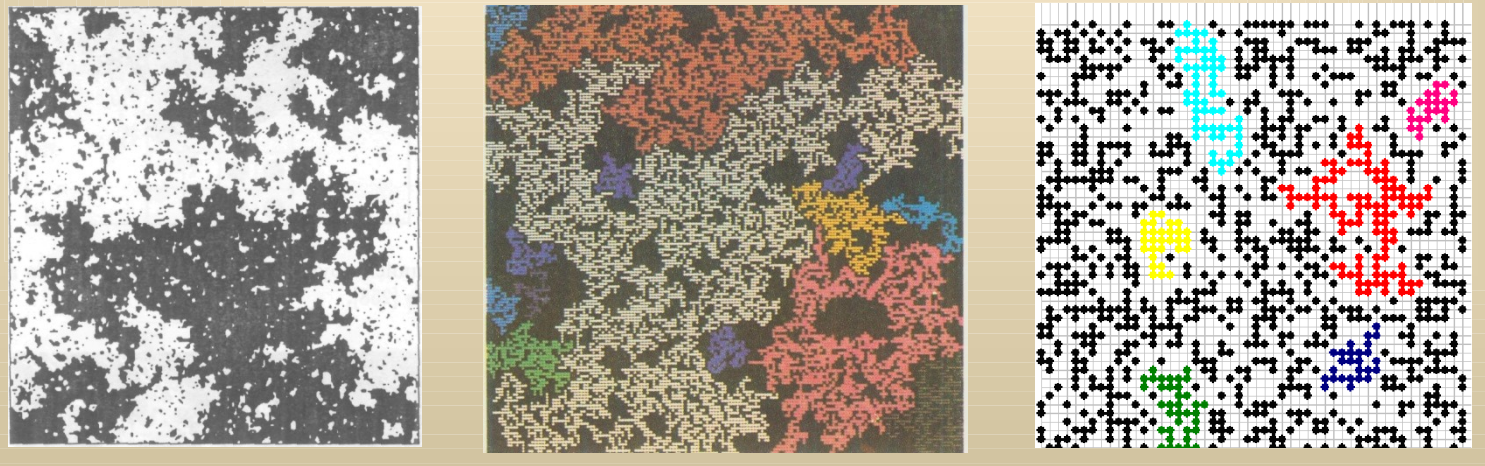

Recovered three-dimensional failure region in copper sample (a); three-dimensional visualization of recovered tantalum sample (b); volume percolation cluster (model calculation) (c)

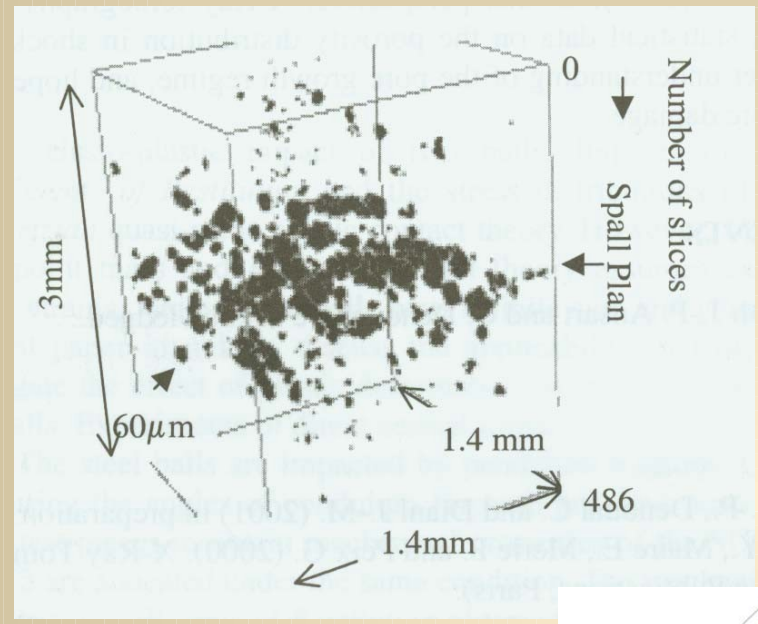

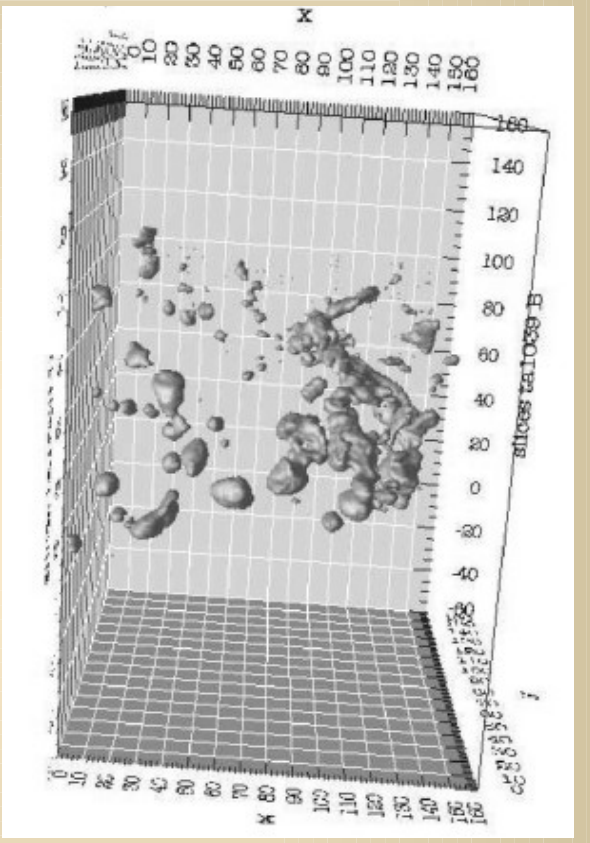

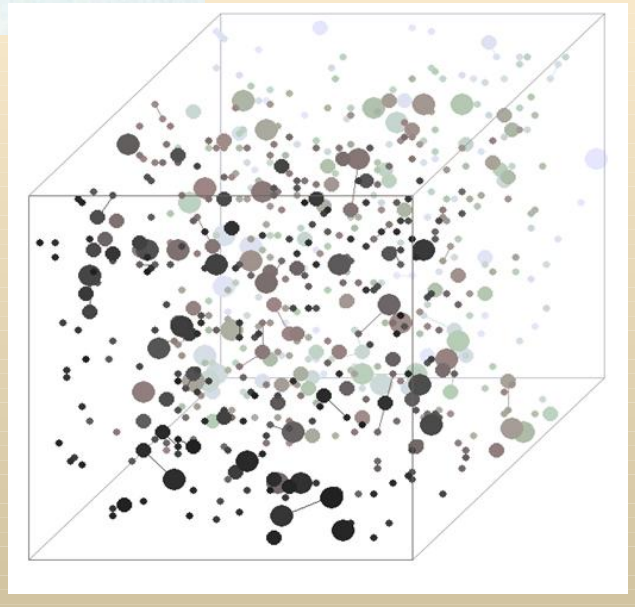

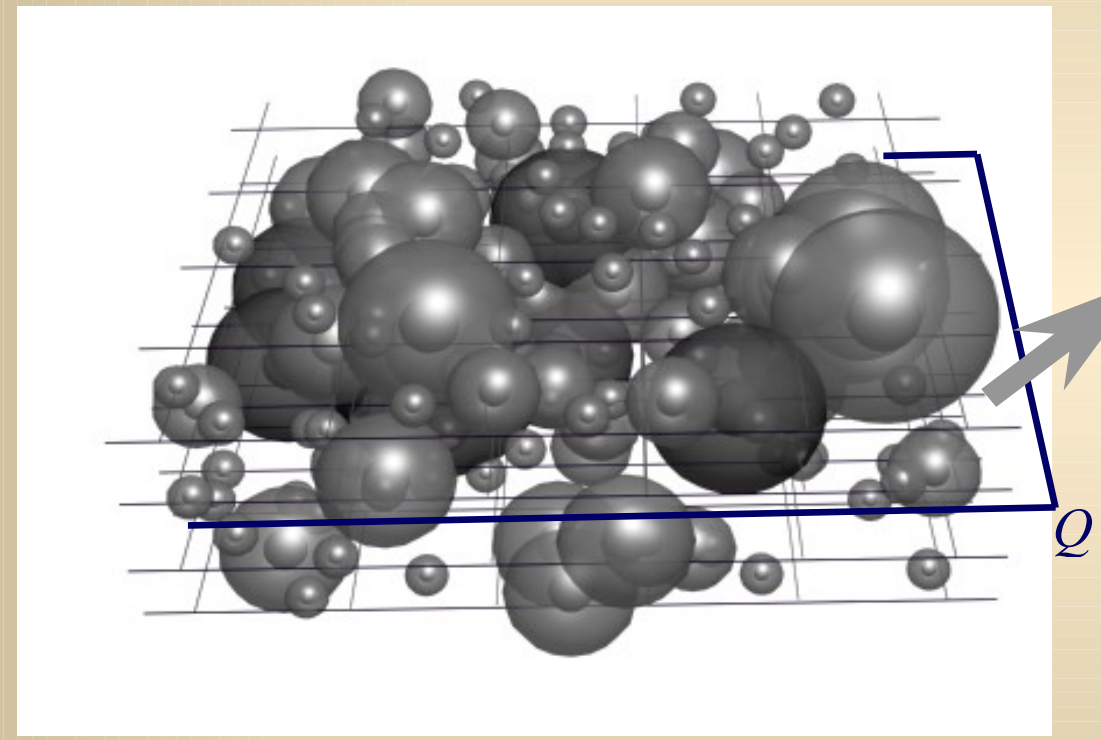
Q

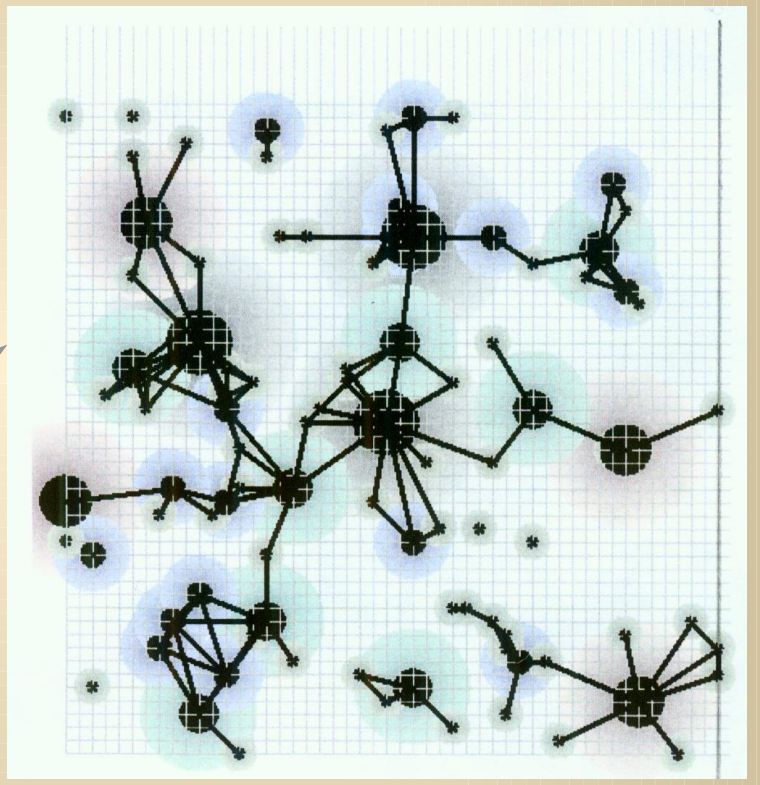

Dependence of average distance between *r=N**(-1/3)* dissipative structure elements on their average size <*D*>. Sizes *r* and <*D*> are given in cm

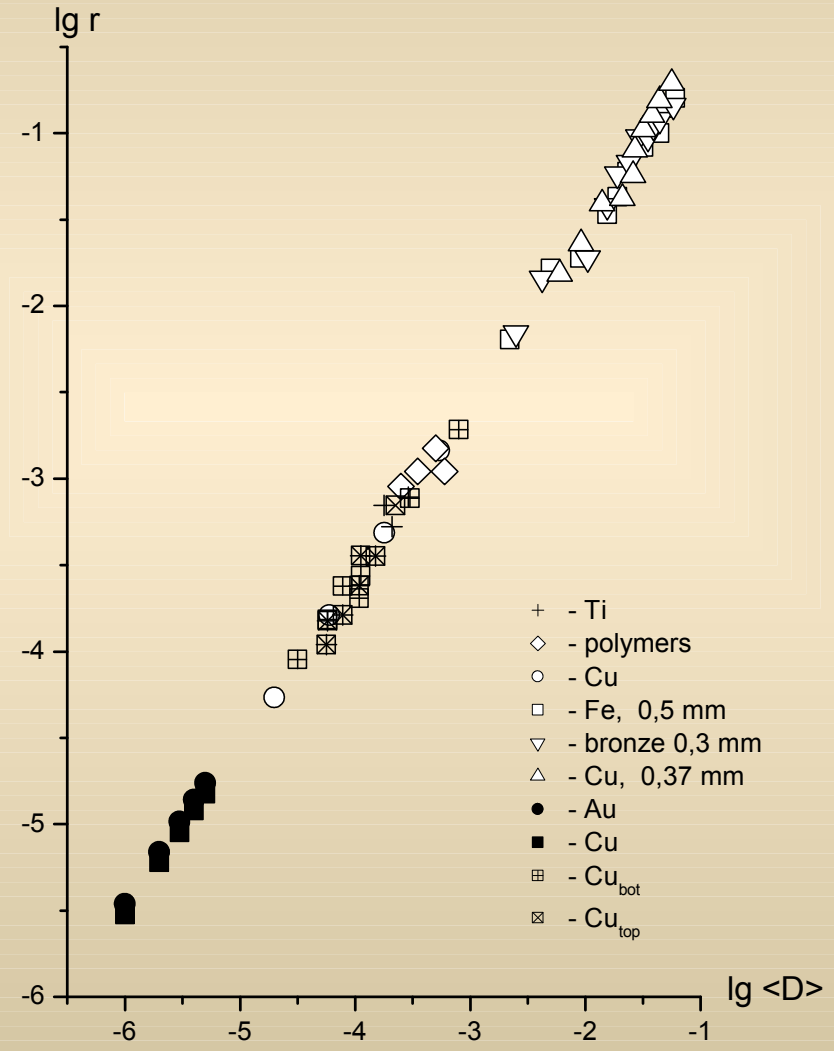

Time dependence of critical pressure and longevity

$$P^{\gamma}(t) \cdot t_r = const,$$

$$\left(\frac{P}{H+L}\right)^{\gamma} t = const \qquad \left(\frac{P}{H+L}\right) = I$$

where γ = 3,8 for all studied materials in the longevity range $t \sim 10^{-6} \div 10^{-10}$ s; t_r – failure time

$$N(t) = N_{tot} \exp\left(\frac{t \cdot I(t_p)}{B}\right)^{0,4} \left(1 - \frac{t \cdot I(t_p)}{B}\right)^{-1,2}$$

$$J(t) = J_{tot}(t_p) \exp\left(\frac{t \cdot I(t_p)}{A}\right)^{0,2} \left(1 - \frac{t \cdot I(t_p)}{A}\right)^{-2,2}$$

where A, B – const

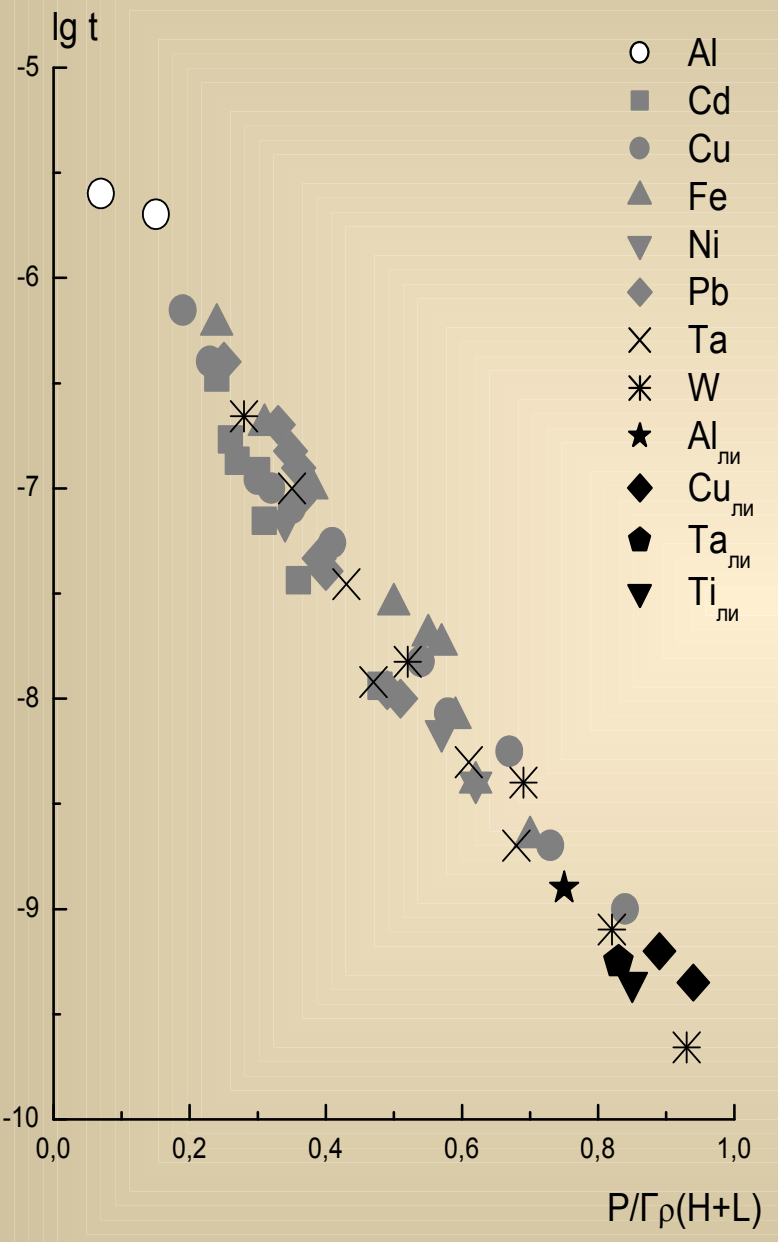
lg t
-5
-6
-7
-8
-9
-10
0,0
0,2
0,4
0,6
0,8
1,0
P/Γρ(H+L)
Al
Cd
Cu
Fe
Ni
Pb
Ta
W
Al ли
Cu ли
Ta ли
Ti ли

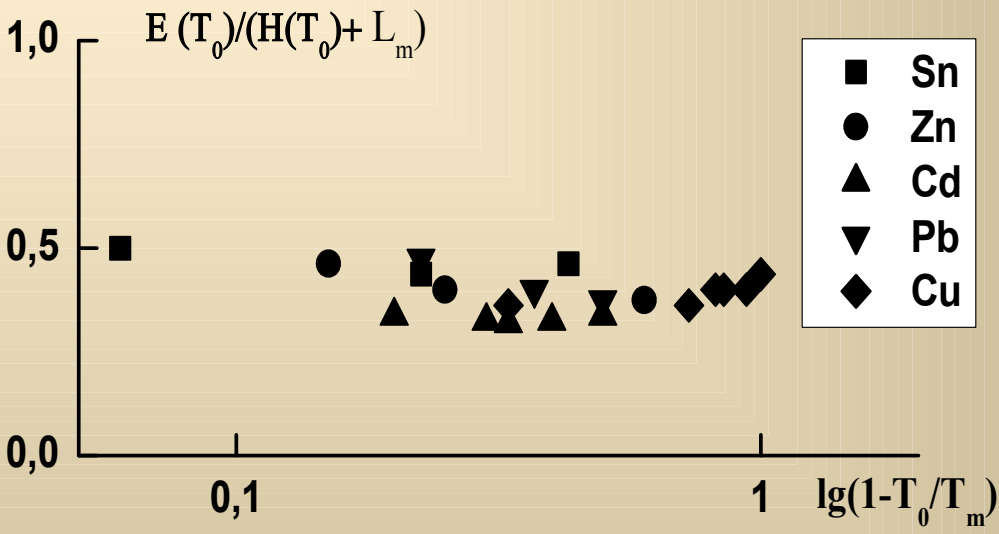
1,0
0,5
0,0
E (T0)/(H(T0)+ Lm)
0,1
1
lg(1-T0/Tm)
Sn
Zn
Cd
Pb
Cu

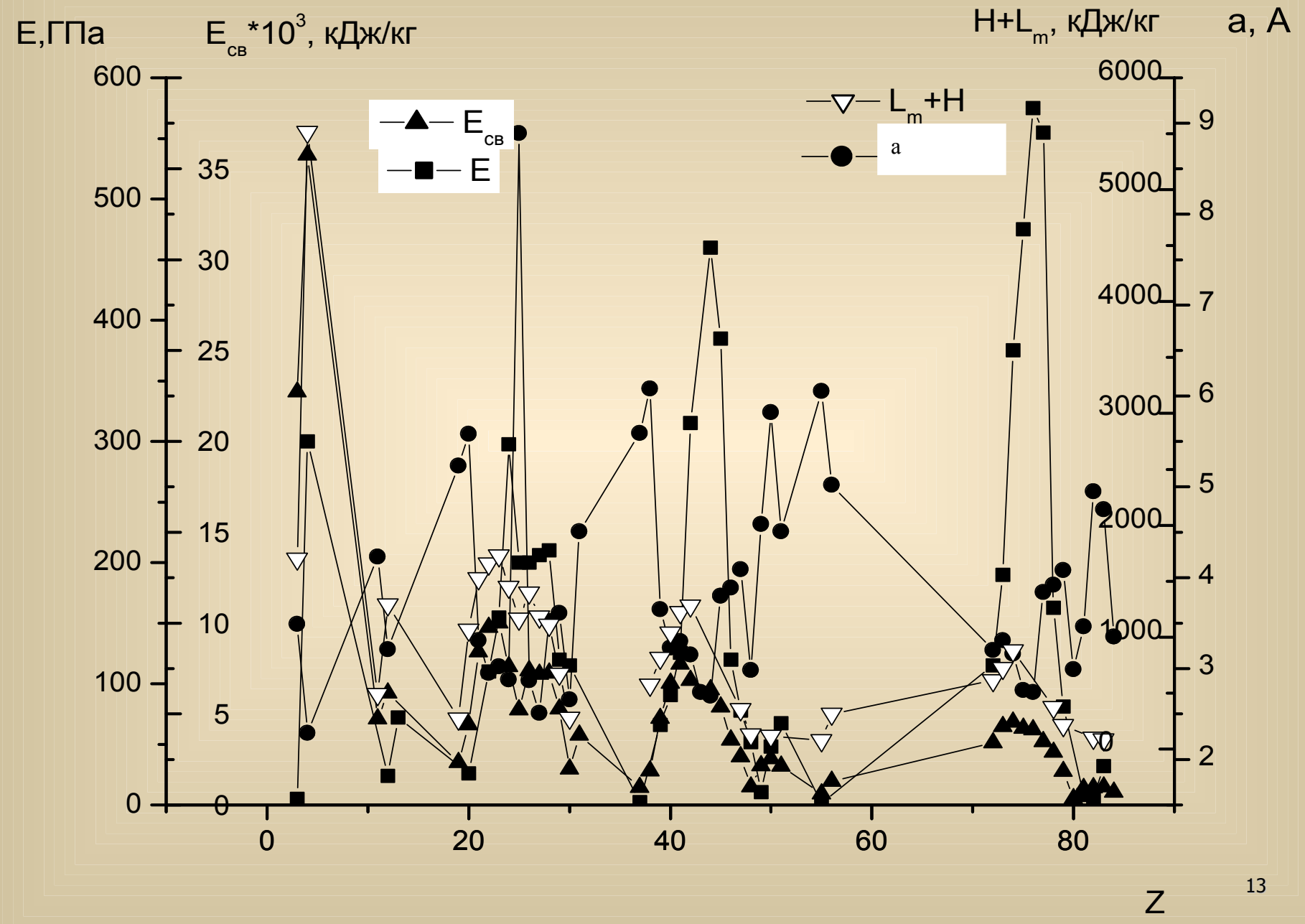
E,ГПа
$E_{св}$*10^3, кДж/кг
H+L_m, кДж/кг
a, A
$E_{св}$
E
L_m+H
a
600
500
400
300
200
100
0
35
30
25
20
15
10
5
0
6000
5000
4000
3000
2000
1000
0
9
8
7
6
5
4
3
2
0
20
40
60
80
Z

$t \sim 10^{-8}$ s

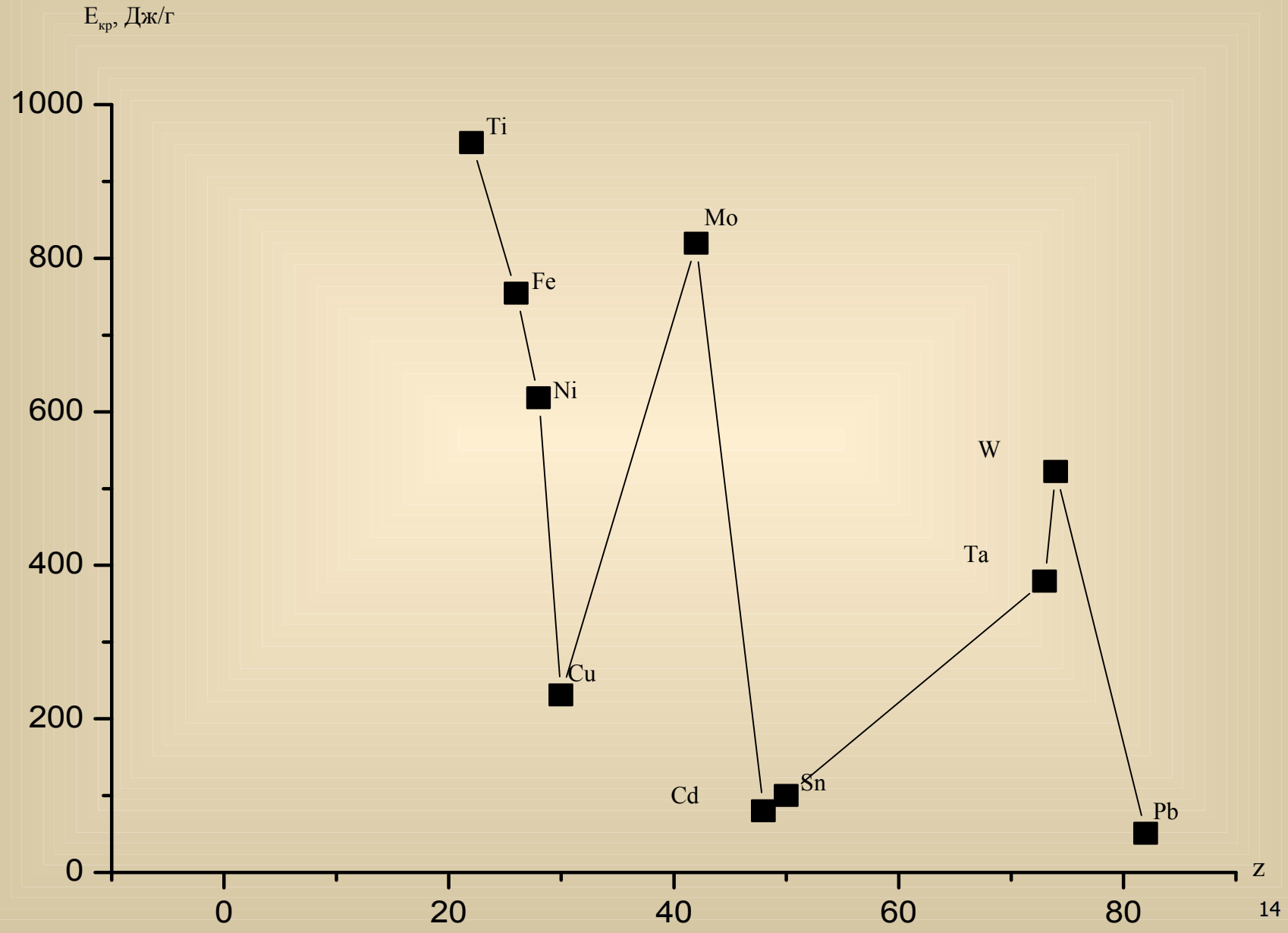
$E_{кр}$, Дж/г
1000
800
600
400
200
0
0
20
40
60
80
z
Ti
Fe
Ni
Cu
Mo
Cd
Sn
Ta
W
Pb

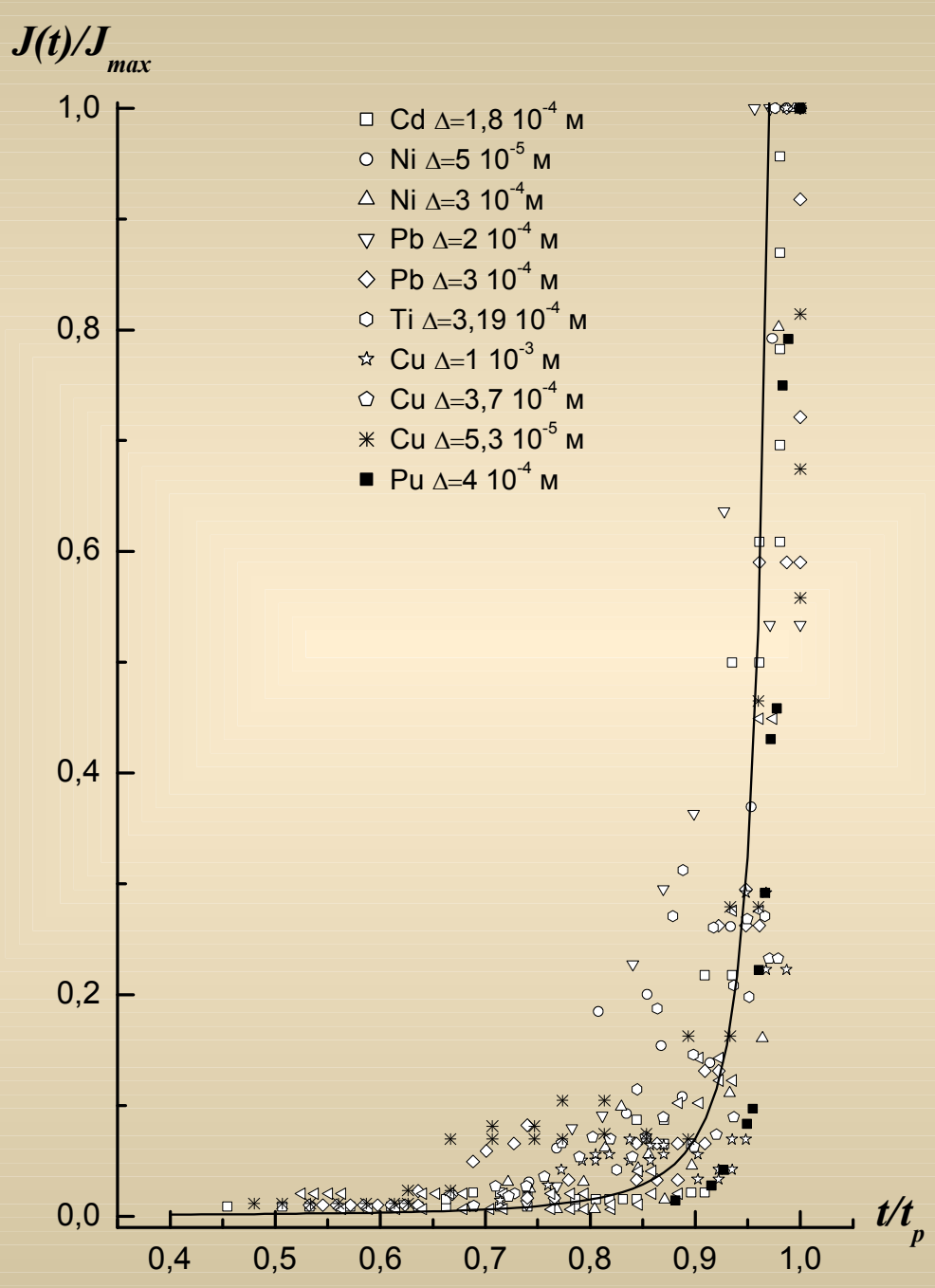
J(t)/J max
1,0
0,8
0,6
0,4
0,2
0,0
0,4
0,5
0,6
0,7
0,8
0,9
1,0
t/t p
Cd Δ=1,8 10-4 м
Ni Δ=5 10-5 м
Ni Δ=3 10-4м
Pb Δ=2 10-4 м
Pb Δ=3 10-4 м
Ti Δ=3,19 10-4 м
Cu Δ=1 10-3 м
Cu Δ=3,7 10-4 м
Cu Δ=5,3 10-5 м
Pu Δ=4 10-4 м

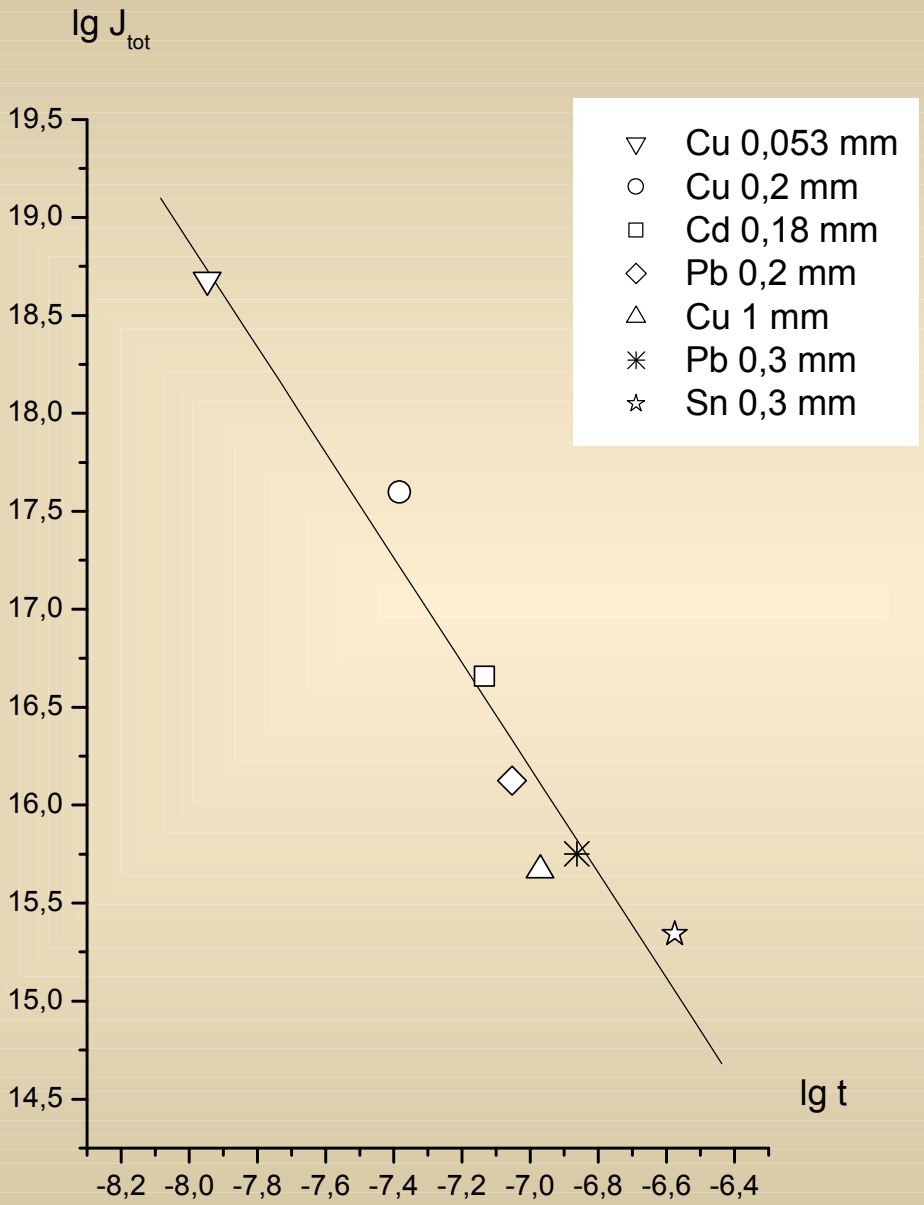
lg J tot
19,5
19,0
18,5
18,0
17,5
17,0
16,5
16,0
15,5
15,0
14,5
-8,2
-8,0
-7,8
-7,6
-7,4
-7,2
-7,0
-6,8
-6,6
-6,4
lg t
Cu 0,053 mm
Cu 0,2 mm
Cd 0,18 mm
Pb 0,2 mm
Cu 1 mm
Pb 0,3 mm
Sn 0,3 mm

$$J(t) \sim t^{-2,5}$$

$$x_0 = \left(\frac{N\hbar}{k\theta M} \right)^{1/2}$$

$$\theta(V) = \theta_0 \left(\frac{v_0 - V}{v_0 - V_0} \right)^2 \left(\frac{V_0}{V} \right)^{2/3}$$

$$A(V) = \left(\frac{N\hbar^2}{K\theta M} \right)^{1/2} \left(\frac{N}{V_0} \right) \left(\frac{v_0 - V_0}{v_0 - V} \right)$$

Dependence of parameter De Bure on specific volume (Al)

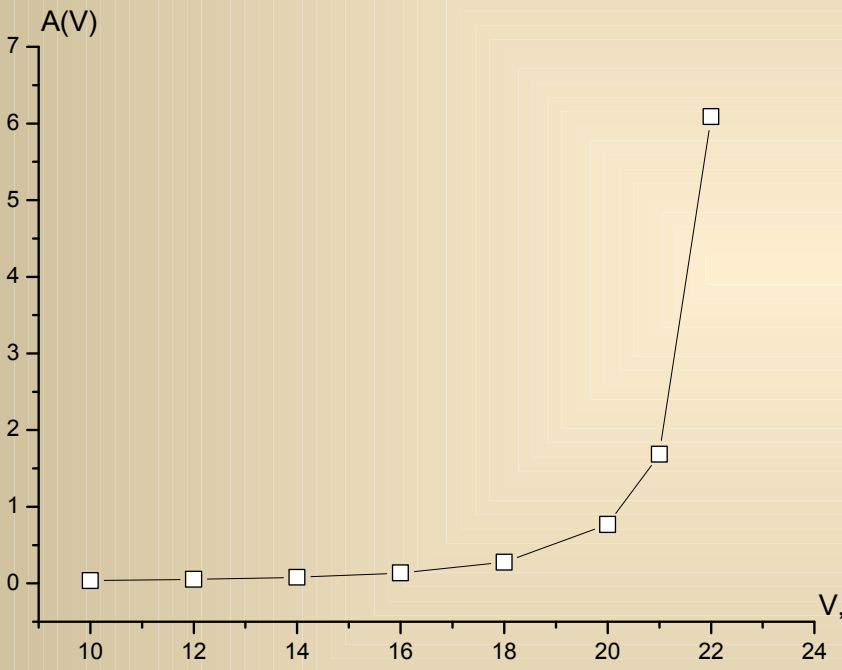

Dependence of effective temperature on specific volume (Al)

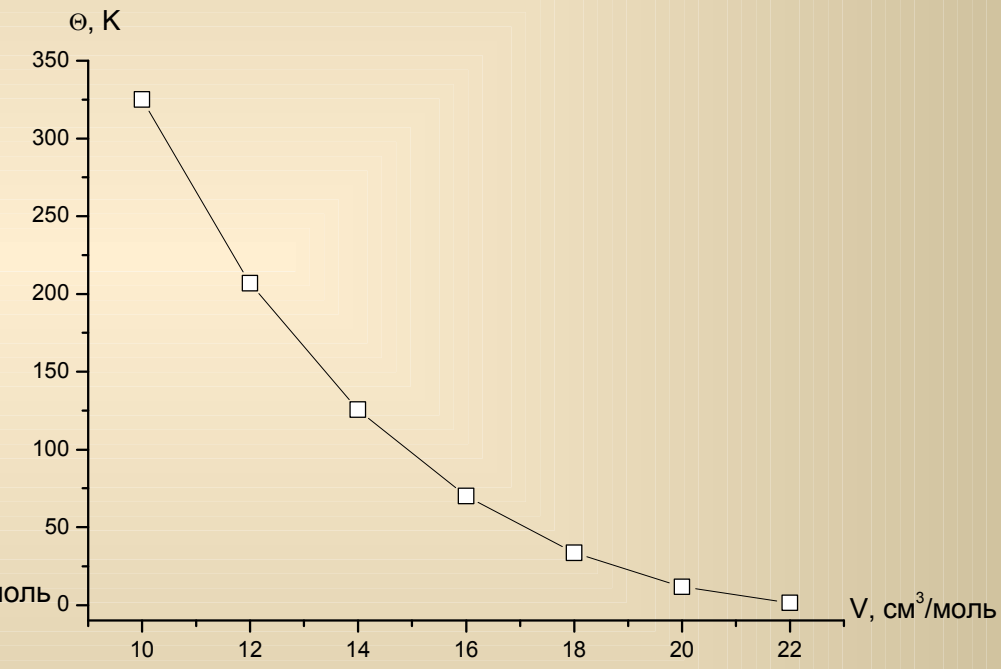

Characteristics of interatomic interactions in metals

Элемент	ат. №	V, 10^{-30} м^3	a, пм	Hs, 10^{-20} Дж/ат	KV, 10^{-20} Дж	$T_{пл}$, К	T_D, К	$\alpha_{пл}$
Al	13	16603	285,77	48,7	127	934	390	0,010
Ti	22	17665	288,98	68,1	189	1941	380	0,014
Fe	26	11776	247,73	58,1	191	1810	373	0,013
Ni	28	10939	248,65	61,4	201	1728	345	0,012
Cu	29	11807	255,08	50,2	163	1358	310	0,011
Zn	30	15212	265,95	19,2	104	693	237	0,009
Mo	42	15580	270,82	96,7	411	2901	337	0,010
In	49	26144	324,46	37,9	110	430	129	0,005
Cd	48	21581	297,28	16,5	115	594	321	0,007
Sn	50	27047	301,6	49,2	150	505	254	0,005
Ta	73	18000	285,0	123,8	348	3269	225	0,013
W	74	15855	273,53	127,9	491	3693	312	0,010
Pb	82	30326	349,32	29,6	136	600	87	0,006

Element, V- Volume per one atom, Interatomic distance, Sublimation heat per atom, Lattice energy unit, K- Compression modulus, $T_{ПЛ}$- Melting temperature, T_D - Debye temperature, Dimensionless melting temperature

Fractography of microstructure of cross-section slice of tungsten foil with thickness Δ = 0.02 mm after irradiation (x500)

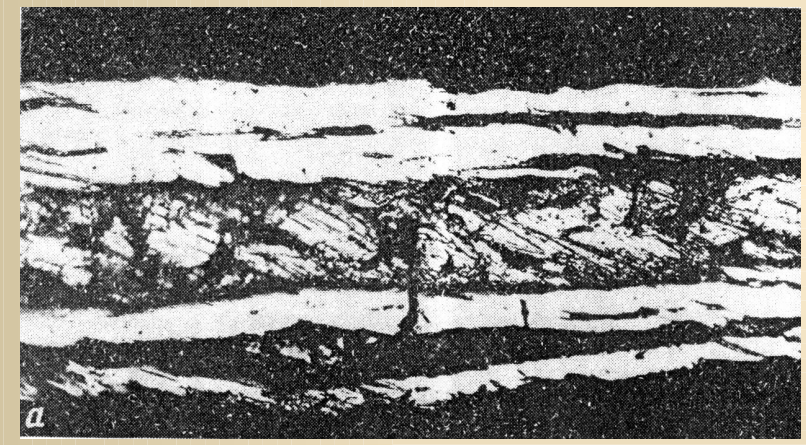

Particle ejection from the free surface of lead sample (roughness Rz40) after shock wave exit – at the time moment 3.8 μs

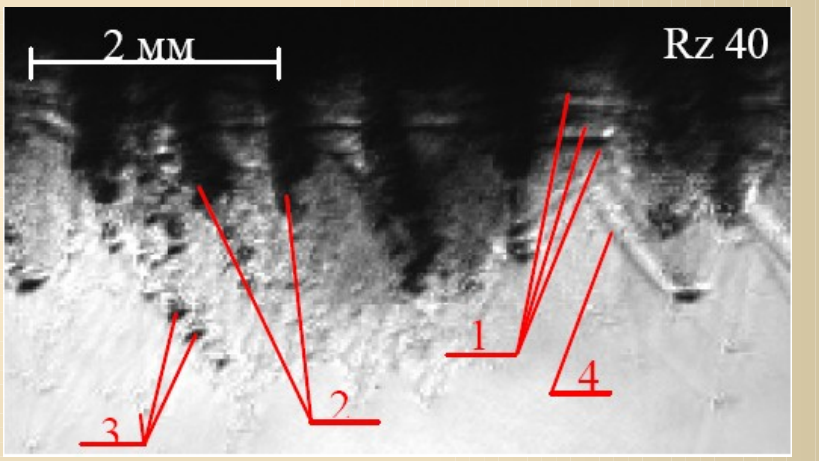

1 – spalls; 2 – micro-jet;
3 – particles; 4 – shock wave in air

View of failed pyramids (a); copper sample slice after REB action (b); disperse products on the obstacle (c); view of disperse metal particles on the obstacle (d); copper pyramid face (x200) (e)

x45

a

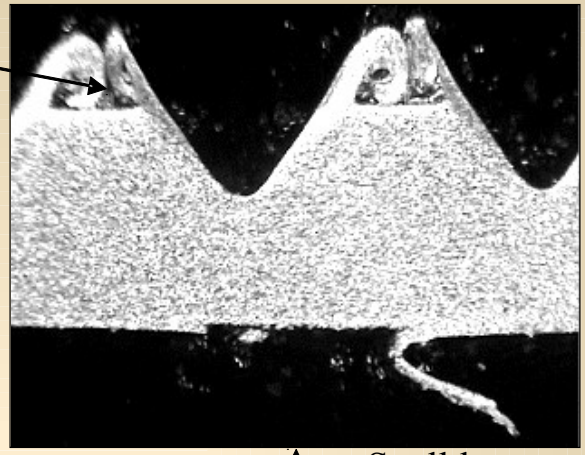

x40

b

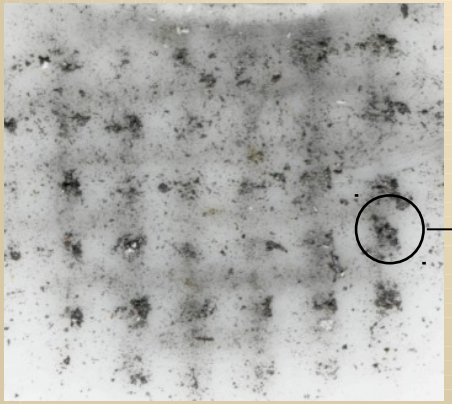

c

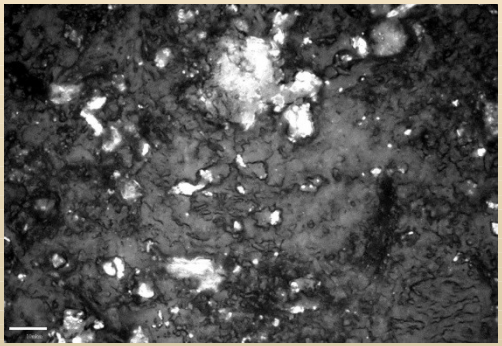

10 μm

d

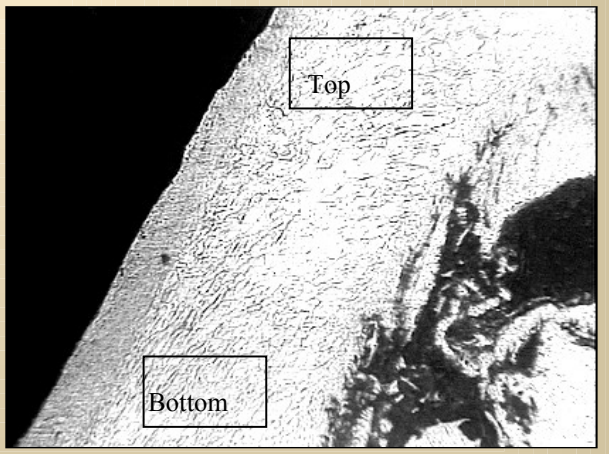

e

External view of copper pyramid face and mathematical treatment of bottom part of copper pyramid

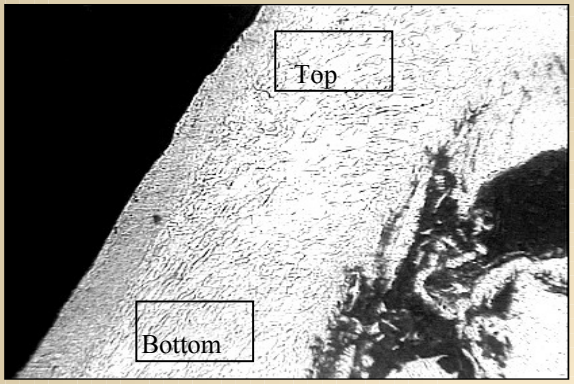

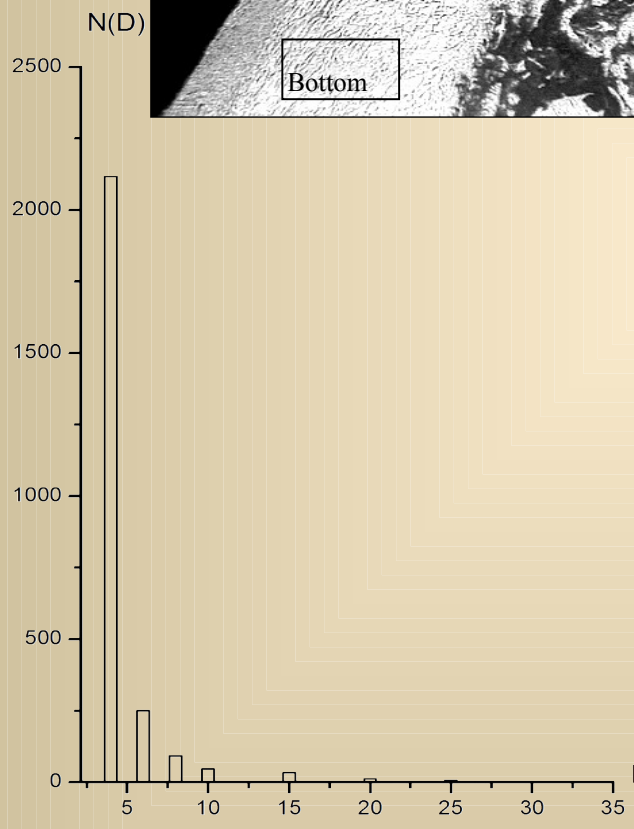

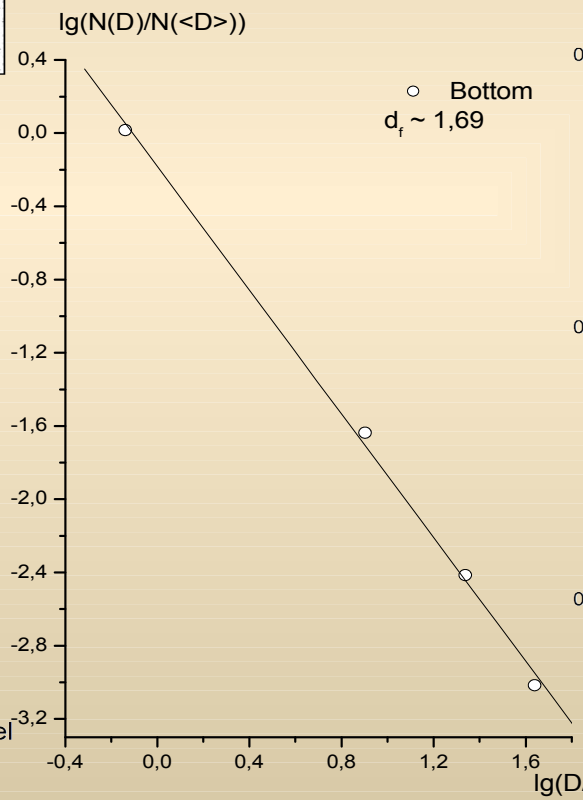

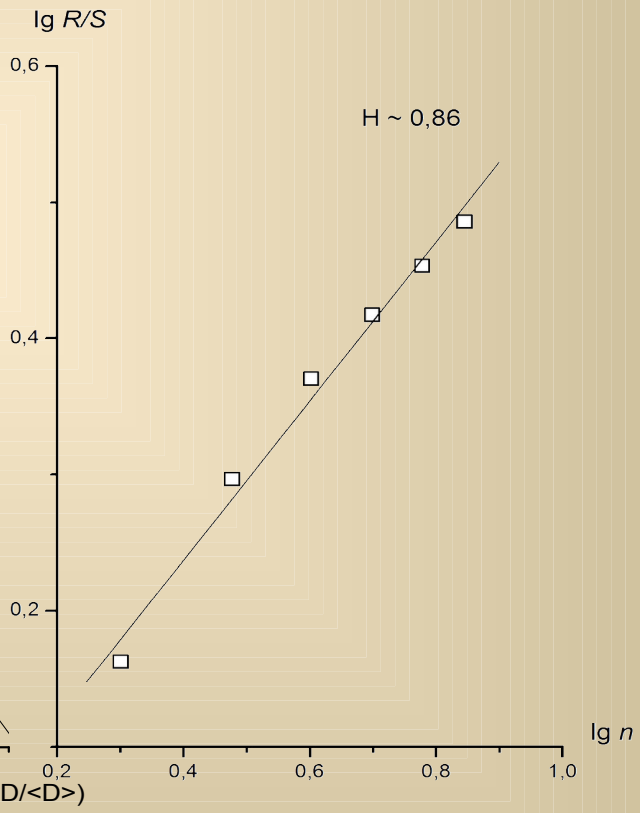

Mathematical treatment of top copper pyramid part

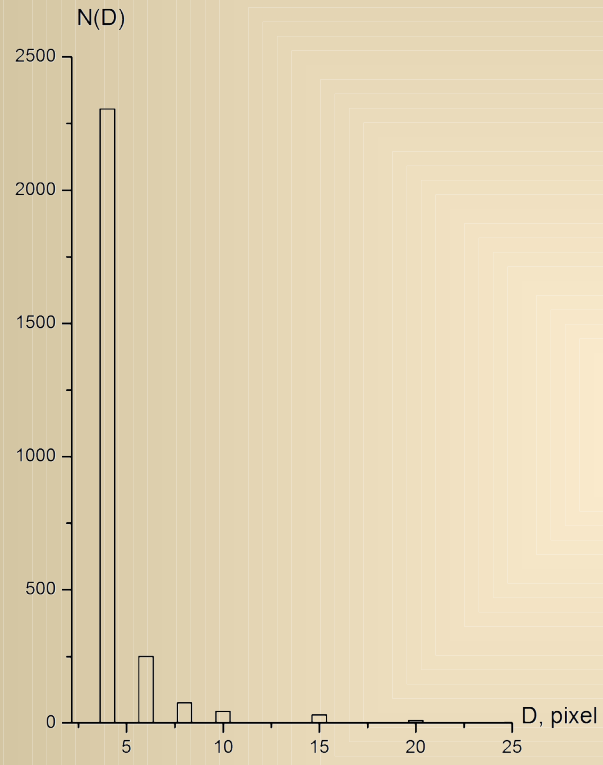

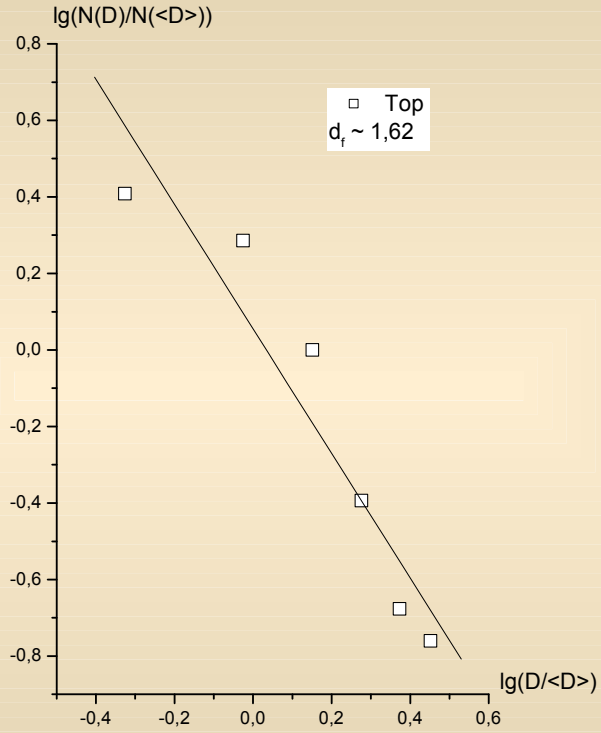

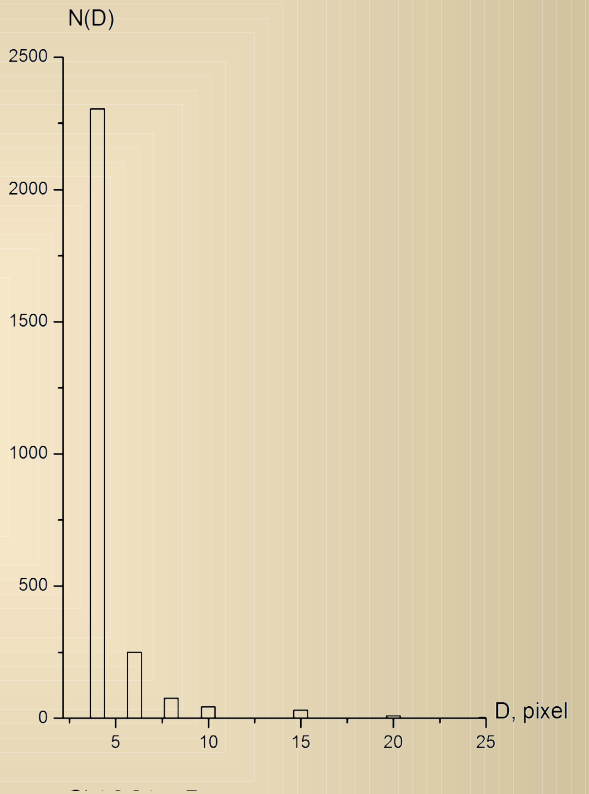

Metal energy parameters

Элемент	ат. №	$\frac{H + L_{пл}}{H_{субл}}$	$E_{кр}$, Дж/г при $t = 10^{-8}$ с	$\frac{E_{кр}}{H + L_{т}}$ при $t = 10^{-8}$ с
Al	13	0,151	–	–
Ti	22	0,16	950	0,537
Fe	26	0,18	754	0,585
Co	27	0,16	–	–
Ni	28	0,15	618	0,533
Cu	29	0,144	394	0,575
Zn	30	0,157	–	–
Mo	42	0,18	819	0,537
Cd	48	0,18	80	0,494
Sn	50	0,12	100	0,525
Ta	73	0,186	379	0,495
W	74	0,165	522	0,570
Pb	82	0,116	51	0,510

Scheme of shock wave motions in the pyramid volume

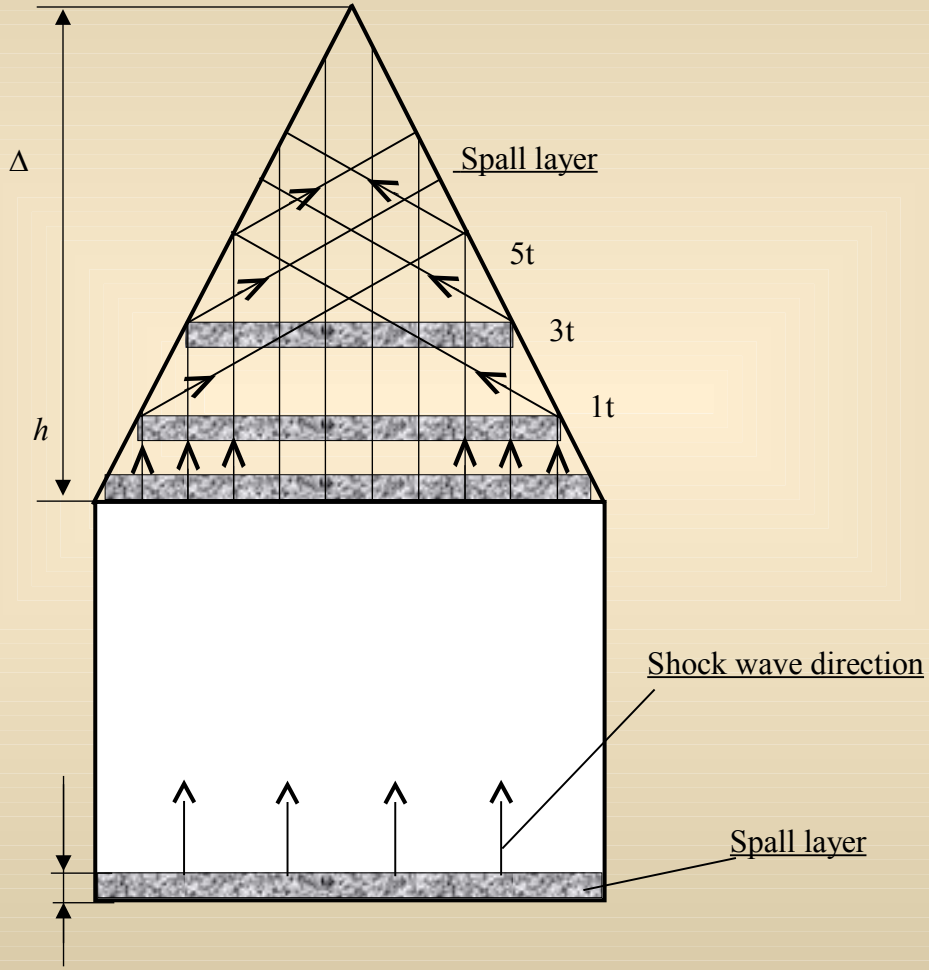

1) Geometrical similarity

$x' = cx,\ y' = cy,\ z' = cz,$

where c – geometrical similarity factor.

2) Field similarities

$\varphi(x, y, z)$ (field of temperature, concentration, potential).

$$\varphi'(x', y', z') = c_\varphi \varphi(x, y, z)$$

3) Process similarities

$$\tau' = c_\tau \cdot \tau$$

$$\varphi'(x', y', z', \tau') = c_\varphi \varphi(x, y, z, \tau),$$

for x', y', z', τ' и x, y, z, τ are related by the correlation

$x' = cx,\ y' = cy,\ z' = cz,\ \tau' = c_\tau \cdot \tau$

Pyramid fragment after loading (x200)

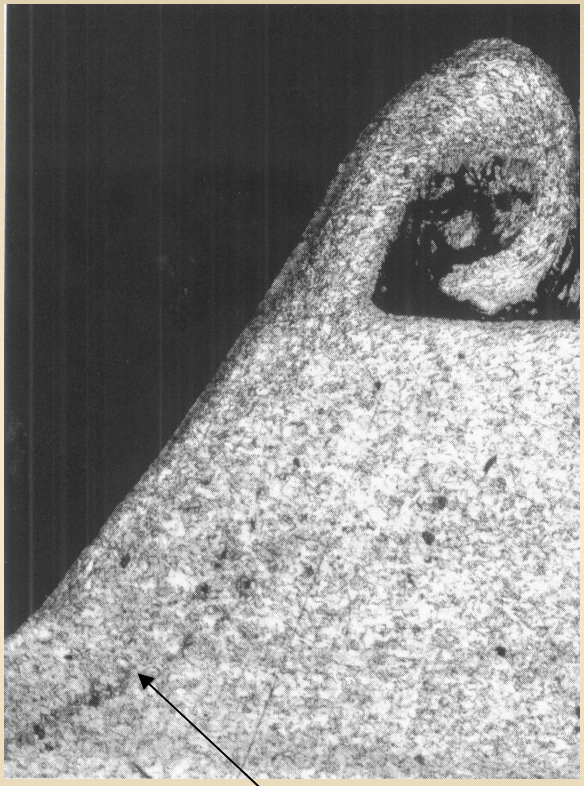

Origin of spall phenomenon near the pyramid faces

External view of disperse particles from the pyramid (Cu, corner angle $\alpha \sim 60^0$) and results of mathematical disperse particles treatment

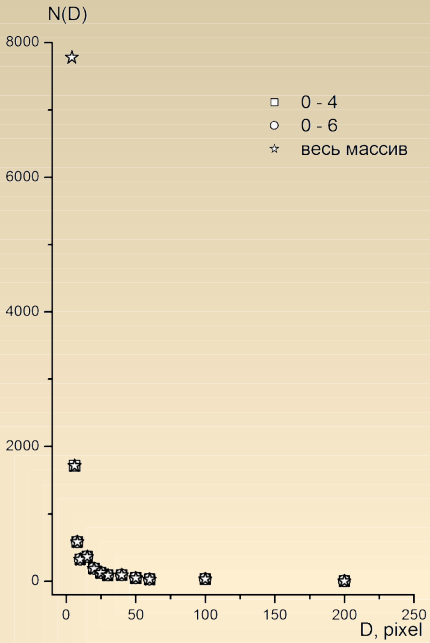

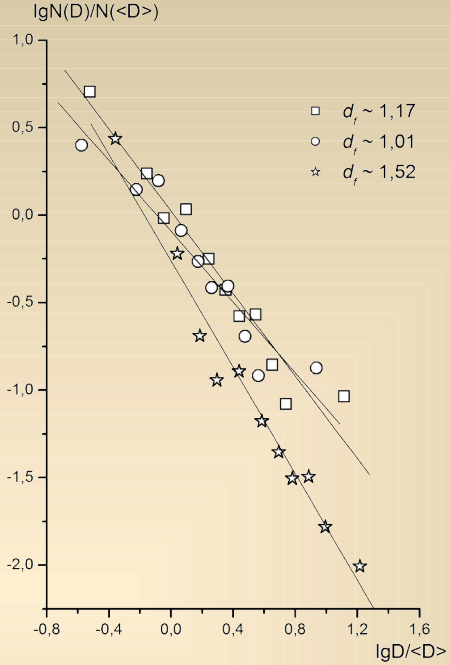

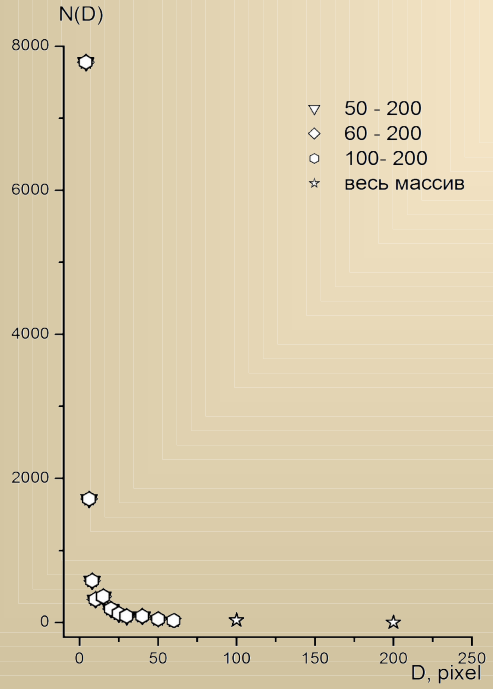

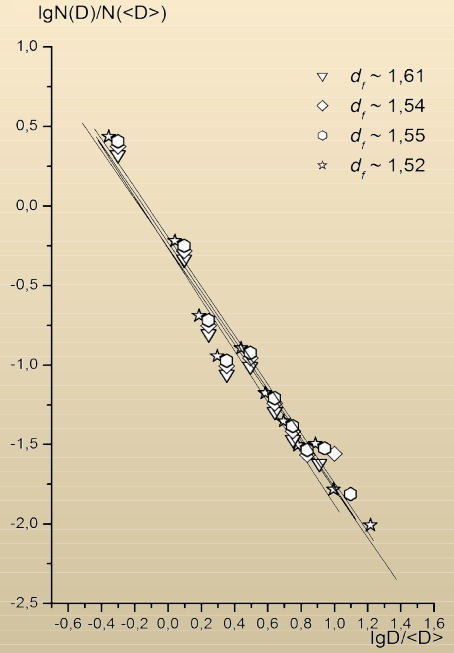

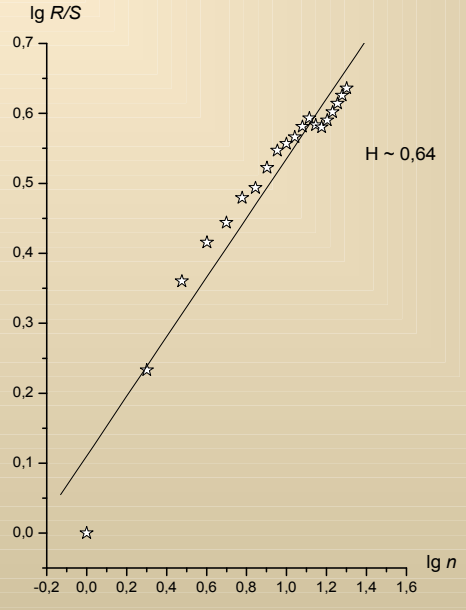

External view of support region made of polyethylene and results of mathematical treatment of disperse particles

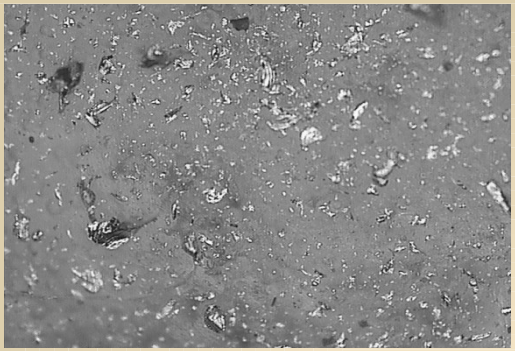

Distance between two big lines is 100 μm

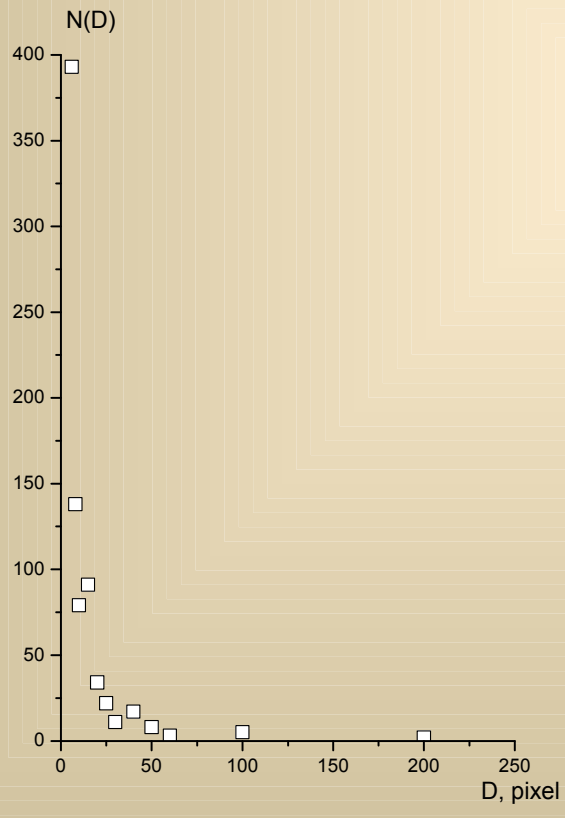

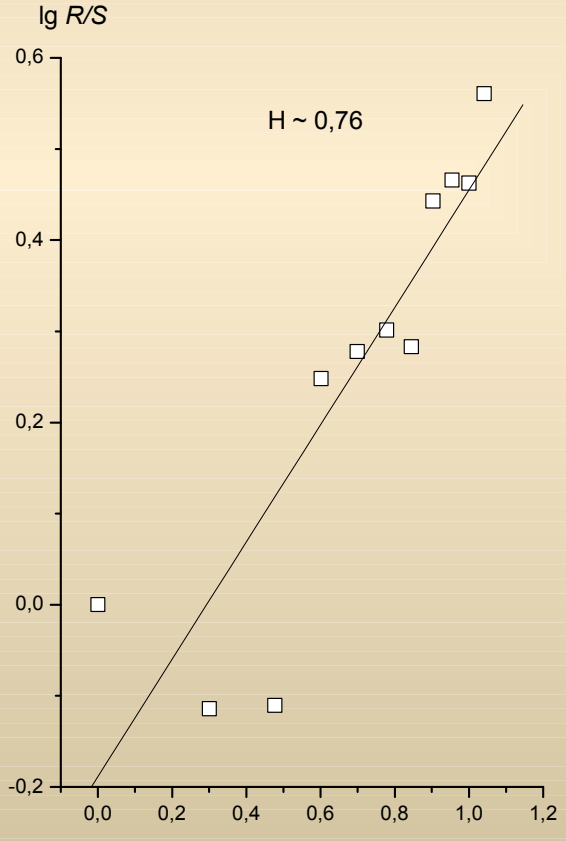

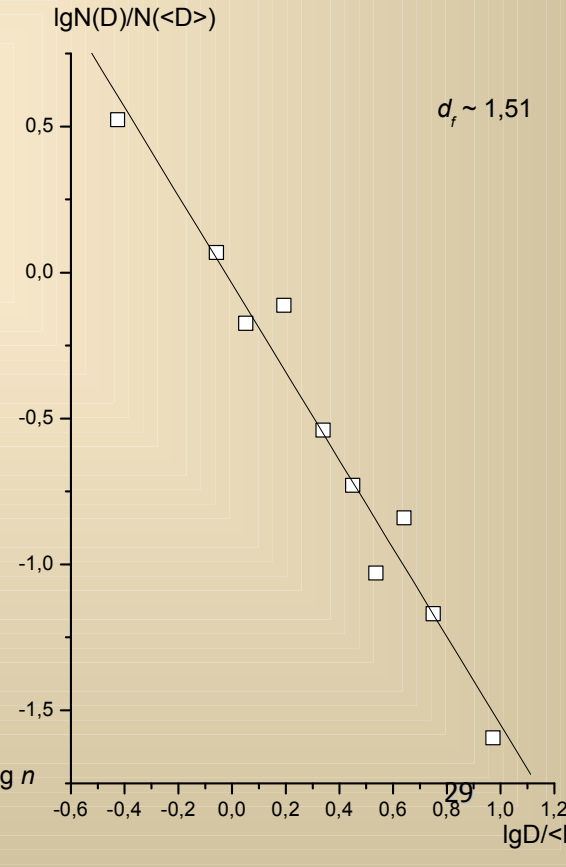

Results of mathematical treatment (d_f) of disperse particles from the pyramids (Al and Cu, corner angle $\alpha \sim 60^0$)

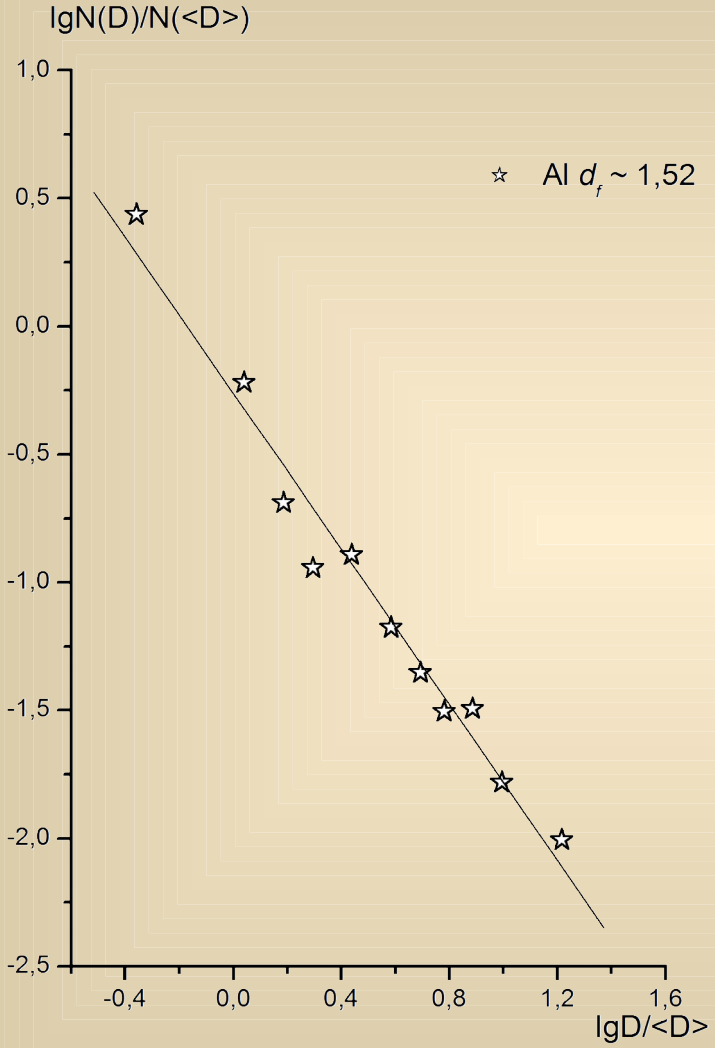

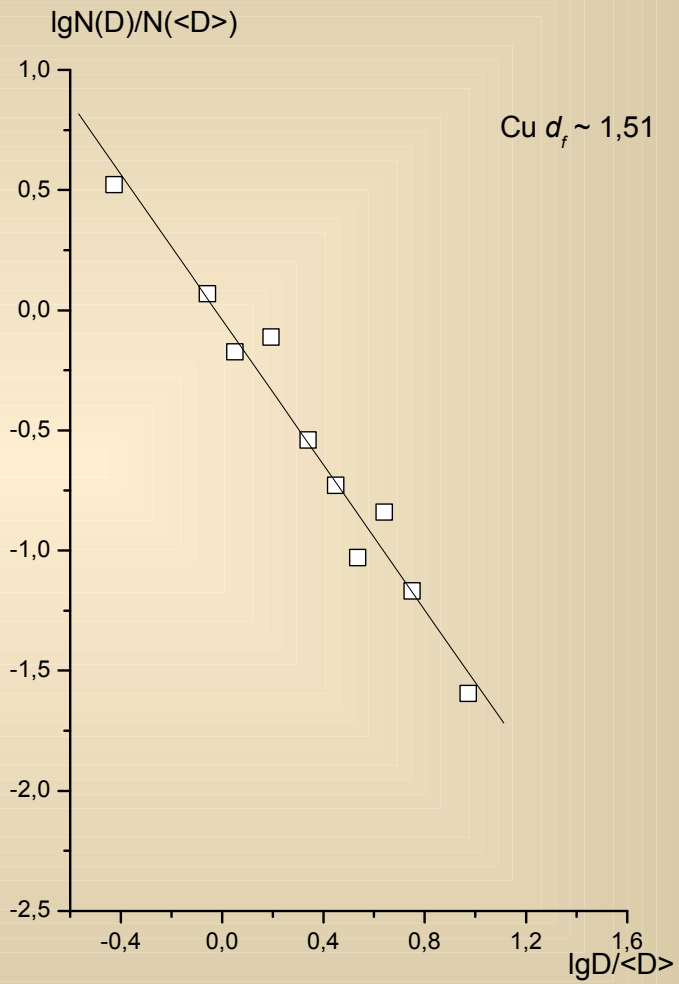

Explosion welding results

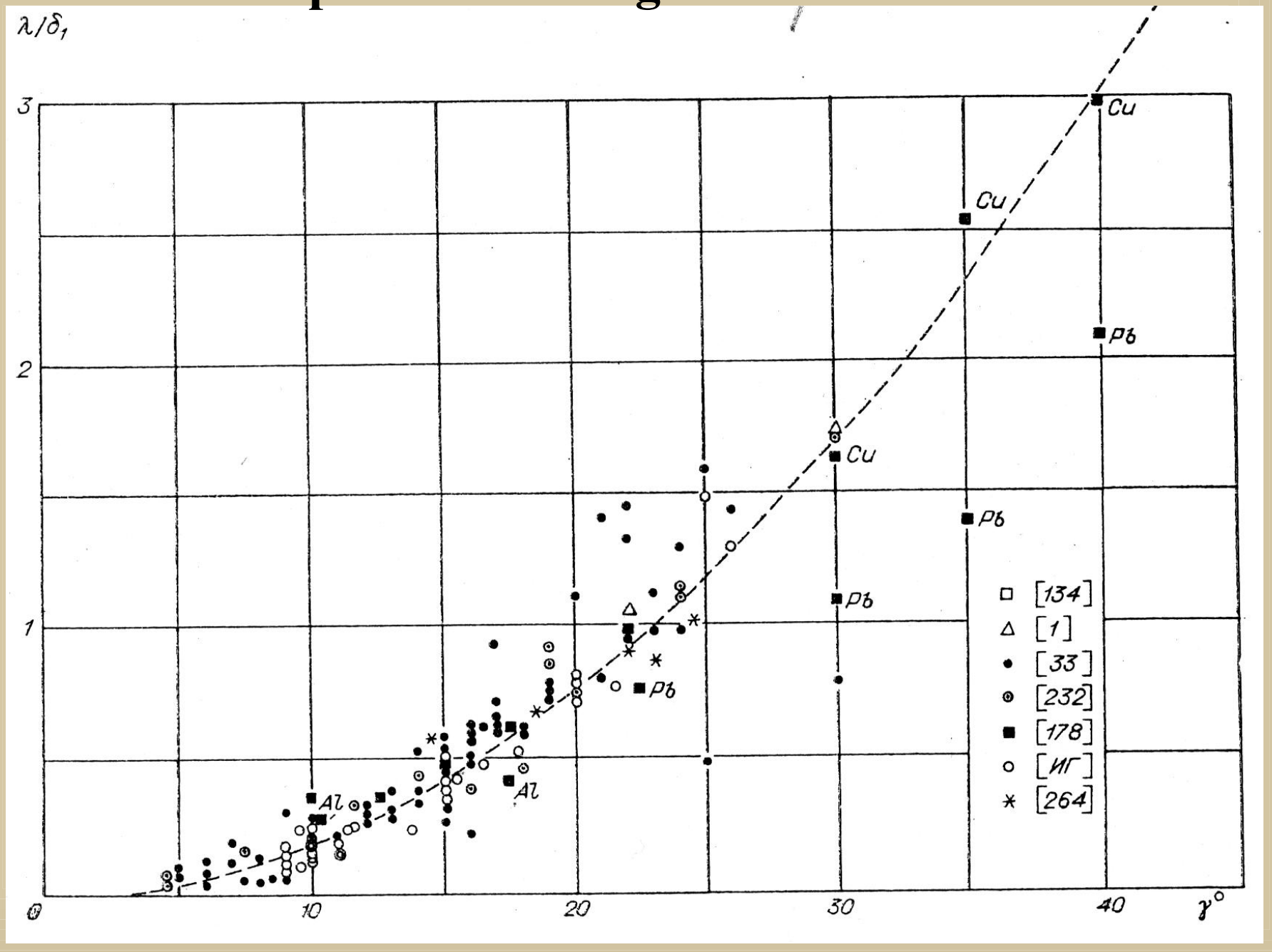

Density distribution (a); in the axial section – (b). Calculation 3D using spall failure. Time 3 μs

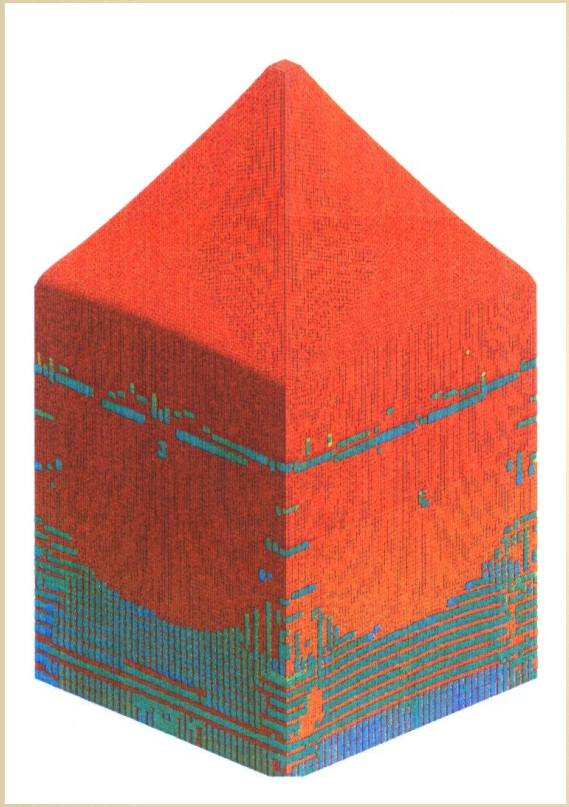

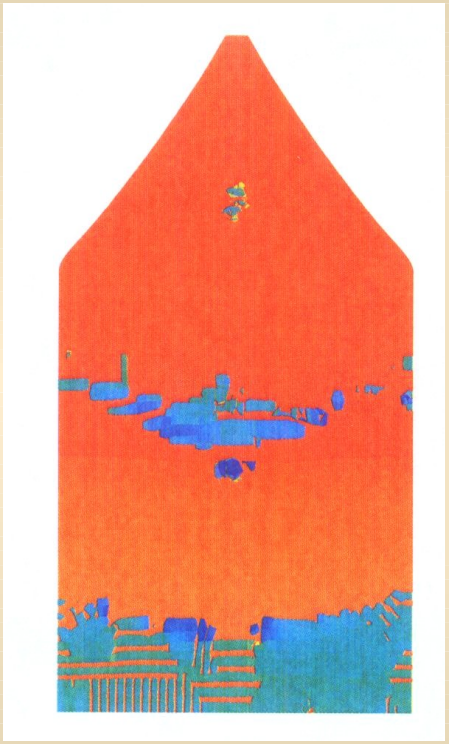

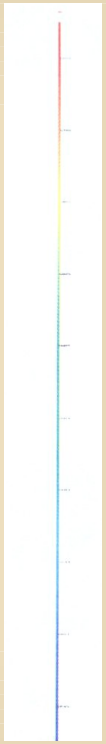

Blue color – practically zero density,
Green color – porous medium.

New kinetic variables of metal dispersion processes are obtained at amplitudes of shock-wave loading $P \sim$ units-tens GPa, what is important for verification of existing calculation codes.

The aforesaid is of much importance for verification of available dynamic state equations and developing of new (adequate) ones, allowing description of metals' behavior under extreme conditions using existing calculation codes.

Results of performed studies are useful when developing new state equations to describe metal behaviors under extreme conditions.

One should take into account presented study results when developing a high-intensity pulse technology.

References:

1. Kinetics of dynamic metals failure in the mode of pulsed volume heat-up. Bonyushkin E.K., Zavada N.I., Novikov S.A., Uchaev A.Ya.. – Sarov, RFNC-VNIIEF, 1998. – 275 p.
2. Kosheleva E.V., Punin V.T., Sel'chenkova N.I., Uchaev A.Ya. Common regularities of hierarchy relaxation processes in metals under the action of penetrating radiation pulses: Monograph - Sarov: RFNC-VNIIEF, 2015. – 211 p.
3. Il'kaev R. I., Uchaev A.Ya., Novikov S.A., Zavada N.I., Platonova L.A., Sel'chenkova N.I. Universal properties of metals in the phenomenon of dynamic failure // DAN, 2002, vol. 384, № 3. – P. 328-333 [in Russian].
4. Il'kaev R. I., Punin V.T., Uchaev A.Ya., Novikov S.A., Kosheleva E.V., Platonova L.A., Selchenkova N.I., Yukina N.A. Time regularities of metals dynamic failure conditioned by hierarchy properties of dissipative structures – failure centers cascade // DAN. 2003. V. 393. № 3. P. 326-331 [in Russian].
5. A.Ya.Uchaev, V.T.Punin, N.I.Selchenkova, E.V.Kosheleva and V.V.Kosachev // Yadernaya Fizika i Inzhiniring. 2014. Vol. 1. № 3. P. 208- 212 [in Russian].
6. A.Ya.Uchaev, V.T.Punin, N.I.Selchenkova, E.V.Kosheleva and V.V.Kosachev Physical nature of light actinides longevity in the dynamic failure phenomenon // Yadernaya Fizika i Inzhiniring. 2014. Vol. 5. № 3. P. 203- 207 [in Russian].
7. A.Ya.Uchaev, V.T.Punin, N.I.Selchenkova, E.V.Kosheleva and V.V.Kosachev Physical nature of light actinides longevity in the dynamic failure phenomenon // Physics of Atomic Nuclei (Fiz. At. Yad.), 2015, №. 12. – P.1-4
8. E.V.Kosheleva, V.V. Mokhova, A.M.Podurets, V.T.Punin, N.I. Selchenkova, A.V.Til'kunov, M.I.Tkachenko, I.R. Trunin, A.Ya.Uchaev Study Of The Processes Of Metals Dispersion Under Shock-Wave Loading Caused By Relativistic Electron Pulses And Accelerated By Liners' Electric Explosion // Physics of Combustion and Explosion, 2017, vol. 53, N2, p. 1-7